Angle-resolved ion-yield measurements of CO_2 in the O $1s$ to Rydberg excitation region

K. Okada

Department of Chemistry, Hiroshima University, Higashi-Hiroshima 739-8526, Japan

H. Yoshida, Y. Senba, and K. Kamimori

Department of Physical Science, Hiroshima University, Higashi-Hiroshima 739-8526, Japan

Y. Tamenori and H. Ohashi

SPring-8/Japan Synchrotron Radiation Research Institute, Sayo-gun, Hyogo 679-5198, Japan

K. Ueda*

Institute of Multidisciplinary Research for Advanced Materials, Tohoku University, Sendai 980-8577, Japan

T. Ibuki

Kyoto University of Education, Fushimi-ku, Kyoto 612-8522, Japan

Angle-resolved energetic-ion-yield spectra were observed in the region of the O $1s$ to Rydberg excitation of CO_2 with incident photon energy resolving power $E/\Delta E \simeq 14\,000$. The assignments of the electronic states were established in accordance with the angular distribution data. All the observed vibrational structures were assigned to the antisymmetric stretching vibrations caused by the vibronic coupling between the nearly degenerate O $1s$ core-excited states. A Franck-Condon analysis was performed within the linear coupling model.

PACS number(s): 33.20.Rm, 33.20.Tp, 33.70.−w

I. INTRODUCTION

Extensive studies of inner-shell absorption and/or electron energy-loss spectroscopy of gas-phase molecules have been performed to obtain information about the electronic structures of the inner-shell excited states [1–3]. The assignments of features observed in these inner-shell spectra, however, have not always been clear even for well-studied simple molecules, because the spectral resolution was not sufficient to give unambiguous assignments of the spectral features, and to obtain information about the vibrational structures. The remarkable progress in soft x-ray monochromator performance in recent years has provided spectra with fine structure and makes it possible to analyze what was not visible at low-energy resolution (for example, see Refs. [4–7]).

The angle-resolved yield spectroscopy of fragment ions provides information about the symmetry of the inner-shell excited state of a linear molecule [8–10], because the intensity of ions ejected in directions parallel and perpendicular to the electric vector of linearly polarized light directly reflects the strengths of the $\Sigma \rightarrow \Sigma$ and $\Sigma \rightarrow \Pi$ transitions, respectively. This type of measurement, called *symmetry-resolved absorption spectroscopy* [11,12], relies on the fact that the core-hole decay and fragmentation occur much faster than molecular rotation, and thus the axial-recoil approximation [13–15] is valid. This technique, combined with a high-resolution monochromator on an undulator beamline which provides linearly polarized light, allows us to make unambiguous assignments of the symmetries of the Rydberg states, as well as probing vibronic couplings in the excited

states (for example, see Ref. [16] and references therein).

In the present work, we applied this technique to the excitation of CO_2 O $1s$ into Rydberg orbitals with the highest energy-resolving power yet employed: $E/\Delta E \simeq 14\,000$. The angle-resolved ion-yield spectra of CO_2 in the C $1s$ and O $1s$ regions were measured by Adachi *et al.* with a resolving power $\simeq 7000$ [17,18]. Bozek *et al.* [19] recorded the O $1s$ spectra at much lower resolving power, $\simeq 150$. The photoabsorption spectra in the C $1s$ and O $1s$ regions were measured by Prince *et al.* [20] with resolving power $\simeq 10\,000$.

The ground-state electronic configuration of the CO_2 molecule is

$$1\sigma_g^2 \ 1\sigma_u^2 \ 2\sigma_g^2 \ 3\sigma_g^2 \ 2\sigma_u^2 \ 4\sigma_g^2 \ 3\sigma_u^2 \ 1\pi_u^4 \ 1\pi_g^4 \quad (^1\Sigma_g^+), \tag{1}$$

where $1\sigma_g$ and $1\sigma_u$ are linear combinations of the two O $1s$ orbitals and $2\sigma_g$ is the C $1s$ orbital. Dipole-allowed absorption of the Σ_g ground state leads to the Σ_u and Π_u states. The dipole transition moments are parallel and perpendicular to the molecular axis for the $\Sigma_g \rightarrow \Sigma_u$ and $\Sigma_g \rightarrow \Pi_u$ transitions, respectively. The O $1s$ $1\sigma_g$ electron can be excited to σ_u and π_u and the O $1s$ $1\sigma_u$ electron to σ_g and π_g, in the absence of vibronic coupling. There are three vibrational modes in the CO_2 molecule ($D_{\infty h}$ symmetry); the symmetric stretching mode ν_1 of σ_g symmetry, the bending mode ν_2 of π_u symmetry, and the antisymmetric stretching mode ν_3 of σ_u symmetry. Vibronic coupling due to the antisymmetric stretching vibration ν_3 (σ_u) is expected to become active between the nearly degenerate electronic states with a hole in $1\sigma_g$ or $1\sigma_u$. This vibronic coupling in CO_2 has been extensively discussed in analyses of the O $1s$ photoelectron spectra [21–23] and the O $1s$ resonant soft x-ray emission spectra [24–26] in CO_2.

─────────
*Corresponding author.
Electronic address: ueda@tagen.tohoku.ac.jp

II. EXPERIMENT

The experiments were performed on the c branch of the soft x-ray photochemistry beamline BL27SU at SPring-8 [27]. This beamline has a figure-8 undulator as a light source. It provides linearly polarized soft x rays [28]. The electric vector E of the first-order harmonic photons lies in the horizontal direction ($0°$), and that of the 0.5th-order light is vertical ($90°$). A monochromator has three varied-line-space gratings and covers the energy region between 150 eV and 3 keV [29]. The energy-resolving power achieved in the O $1s$ region is $\simeq 14\,000$, i.e., the bandpass $\simeq 40$ meV.

The experimental setup and procedure were the same as those in the previous study [30]. In brief, we have simultaneously acquired the energetic-ion-yield curves by using two energetic-ion detectors mounted at $0°$ and $90°$ with respect to the electric vector of the synchrotron radiation [31]. An electrostatic voltage of $+6$ V was supplied in front of the ion detectors in order to detect ions with kinetic energies higher than 6 eV. The sample gas was introduced coaxially with the photon beam by use of a gas nozzle positioned downstream. We repeated the measurements by switching the direction of the E vector from horizontal to vertical and vice versa only by tuning the gap of the undulator. In this way we obtained the angle-resolved ion-yield spectra by measuring the ion intensities ejected in the $0°$ and $90°$ directions after compensating the difference in efficiencies of the two detectors.

The total-ion yield was simultaneously measured with the energetic-ion-yield spectra. The total-ion detector, which was supplied with an extraction field of 500 V/cm, was installed 250 mm upstream from the energetic-ion detectors along the incident photon beam. The photon energy scale was calibrated internally, referring to the published data by Prince *et al.* [20]. Carbon dioxide for the present study was purchased from Showa Tansan Co., Ltd. (99.9990 vol % purity) and used without further purification.

III. RESULTS AND DISCUSSION

A. Symmetry-resolved spectra

Figure 1 shows the ion-yield spectra of CO_2. Panel (a) indicates the total-ion yield and the energetic-ion ($\geqslant 6$ eV) yields, $I(0°)$ and $I(90°)$. The anisotropy parameter β for the energetic ions was obtained from the measured quantities $I(0°)$ and $I(90°)$ by the relation

$$\beta = \frac{2[I(0°) - I(90°)]}{I(0°) + 2I(90°)}. \tag{2}$$

The values of β thus obtained are plotted in panel (b). Under the axial-recoil approximation [13–15], the observed anisotropy of fragmentation directly reflects the initial anisotropy created by the excitation process. It should, however, be remembered that the measured β values include the contributions not only from the O $1s$ excitation but also from the ionization of the valence orbitals as well as the C $1s$ continuum component.

The resolution of the total-ion-yield spectrum in the present work is higher than that published by Prince *et al.* [20]. The spectrum shows some complex structures, which
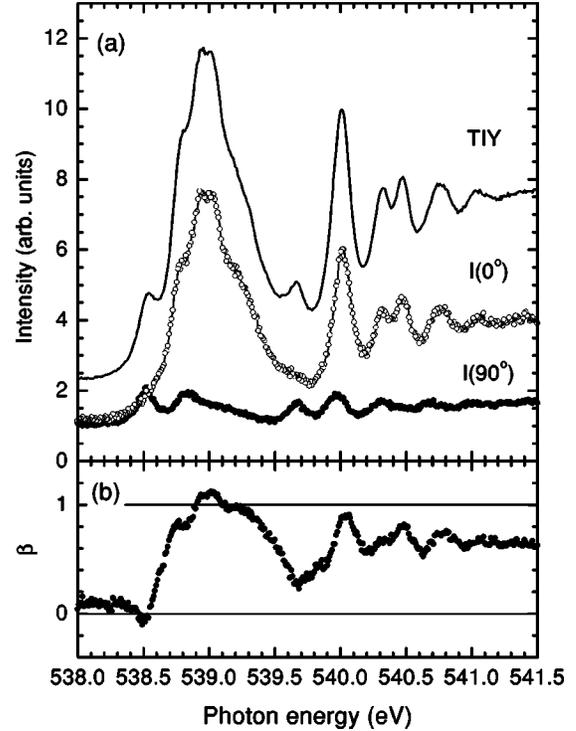

FIG. 1. The yield spectra and the anisotropy parameter β of photofragment ions of CO_2 in the region of the O $1s$ excitation to the Rydberg states. (a) Total-ion-yield spectrum and angle-resolved ion-yield spectra. (b) The β values of the energetic ions ($\geqslant 6$ eV).

allowed Prince *et al.* to propose only tentative assignments. The angle-resolved yield spectra can reduce the complexity as seen in the $I(0°)$ and $I(90°)$ spectra in Fig. 1, and make unambiguous assignments possible. It should be noted, however, that the separation of the $\Sigma \to \Sigma$ and $\Sigma \to \Pi$ transitions is not perfect in the $I(0°)$ and $I(90°)$ spectra, partly because of the finite acceptance angles of the detectors and partly because of the zero-point bending motion of the triatomic molecule. In the vicinity of the 538.8 eV peak, the intensity of the $I(0°)$ spectrum is six times higher than that of the $I(90°)$ spectrum and thus the $I(90°)$ spectrum may include some contributions from the $\Sigma \to \Sigma$ transition. A tail in the region 539.0–539.5 eV is attributed to such contamination due to overlapping of the $\Sigma \to \Sigma$ transition.

The contamination can be eliminated by lowering the amplitudes of the anisotropy parameter for the $\Sigma \to \Pi$ and $\Sigma \to \Sigma$ transitions, β_Π and β_Σ, respectively, under the condition $\beta_\Pi = -0.5\beta_\Sigma$. The prescription is as follows. The measured β values can be expressed by a weighted average of the $\Sigma \to \Sigma$ and $\Sigma \to \Pi$ transitions:

$$\beta = \frac{\beta_\Sigma \sigma_\Sigma + \beta_\Pi \sigma_\Pi}{\sigma_t}, \tag{3}$$

where σ_Σ and σ_Π are the cross sections for the $\Sigma \to \Sigma$ and $\Sigma \to \Pi$ transitions, respectively, and $\sigma_t = \sigma_\Sigma + \sigma_\Pi$. From Eq. (3) one obtains

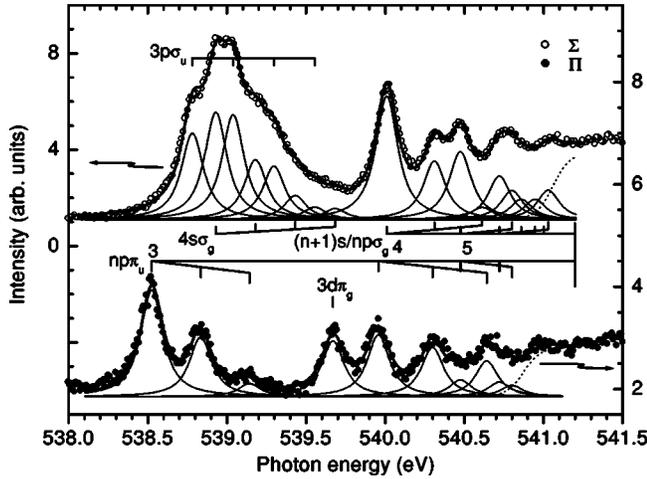$$\sigma_\Pi = \left(\frac{1}{3} \frac{\beta}{\beta_\Pi} + \frac{2}{3} \right) \sigma_t. \tag{4}$$

FIG. 2. Σ and Π spectra and the peak deconvolution analysis. The results of the fit are summarized in Tables I and II.

Adjusting the value of β_Π so as to eliminate the contribution from the $\Sigma \rightarrow \Sigma$ transition in the $I(90°)$ spectrum, we can obtain a pure $\Sigma \rightarrow \Pi$ spectrum using the measured σ_t and β data. We have successfully obtained a pure $\Sigma \rightarrow \Pi$ spectrum with $\beta_\Pi = -0.8$. The resulting spectrum is given by the solid circles in Fig. 2. One can see clearly a new band at 539.1 eV. Similarly, we have obtained a pure Σ spectrum using the relation

$$\sigma_\Sigma = \left(\frac{2}{3} \frac{\beta}{\beta_\Sigma} + \frac{1}{3} \right) \sigma_t \qquad (5)$$

with $\beta_\Sigma = 1.6 \ (= -2\beta_\Pi)$, and plotted by the open circles in Fig. 2.

B. Assignments

To obtain the peak positions as well as the vibrational energy spacing and the intensity of each vibrational component, we have carried out a least-squares peak fitting to the pure Σ and Π spectra, the result of which is shown by the solid lines in Fig. 2. Here each peak is assumed to be represented by a Voigt profile with a Gaussian width of 40 meV and a Lorentzian width of 160 meV. The peak positions thus determined are summarized in Tables I and II together with the proposed assignments.

Let us first focus on the Π spectrum in Fig. 2. The first peak at 538.53 eV corresponds to the excitation to $3p\pi_u$, because the effective principal quantum number of this peak is 2.26. The spacing between this peak and the second peak at 538.83 eV is 0.31 eV. This value is comparable to the frequency $\omega_3 = 307$ meV [22] of the antisymmetric vibration for the O $1s$ ionized state in CO_2. Thus it is reasonable to assign the peak at 538.83 eV to the vibrationally excited component (001) of $3p\pi_u$. Analogously the peaks at 539.96 and 540.30 eV can be assigned to $4p\pi_u(000)$ and $4p\pi_u(001)$. Another prominent peak at 539.67 eV has an effective principal quantum number of 2.98. Thus this peak can be reasonably assigned to $3d\pi_g$.

In Table I all the vibrational components are attributed to the antisymmetric stretching mode ν_3. The vibrational struc-

TABLE I. Π channel Rydberg assignments for CO_2 in the O $1s$ excitation region.

Peak (eV)	Assignment	Term value (eV)	ν (meV)	Quantum defect
538.53	$3p\pi$	2.67		0.74
538.83	$3p\pi(001)$		310	
539.14	$3p\pi(002)$		310	
539.67	$3d\pi$	1.53		0.02
539.96	$4p\pi$	1.24		0.69
540.30	$4p\pi(001)$		340	
540.48	$5p\pi$	0.72		0.66
540.64	$4p\pi(002)$		340	
540.72	$6p\pi$	0.48		0.66
540.80	$5p\pi(001)$		325	
541.20	IP [a]			

[a]Compare 541.254 eV [20].

ture in absorption spectra is usually due to excitation of totally symmetric modes, i.e., the symmetric stretching mode ν_1 in the case of CO_2. The excitation of the antisymmetric stretching mode ν_3 observed here is optically forbidden in the absence of vibronic coupling. The excitation of the O $1s$ core electron, however, leads to symmetry lowering as a consequence of vibronic coupling between the nearly degenerate states of different symmetry, i.e., O $1s \ 1\sigma_g^{-1} np\pi_u$ and O $1s \ 1\sigma_u^{-1} np\pi_u$. As a result, the antisymmetric stretching vibration ν_3 is excited in the core-excited states. The symmetry

TABLE II. Σ channel Rydberg assignments for CO_2 in the O $1s$ excitation region.

Peak (eV)	Assignment	Term value (eV)	ν (meV)	Quantum defect
538.78	$3p\sigma$	2.42		0.63
538.93	$4s\sigma$	2.27		1.55
539.04	$3p\sigma(001)$		255	
539.18	$4s\sigma(001)$		250	
539.30	$3p\sigma(002)$		255	
539.43	$4s\sigma(002)$		250	
539.55	$3p\sigma(003)$		255	
539.68	$4s\sigma(003)$		250	
540.01	$5s/4p\sigma$	1.19		1.62/0.62
540.31	$5s/4p\sigma(001)$		300	
540.48	$6s/5p\sigma$	0.72		1.66/0.66
540.61	$5s/4p\sigma(002)$		300	
540.72	$7s/6p\sigma$	0.48		1.66/0.66
540.80	$6s/5p\sigma(001)$		325	
540.86	$8s/7p\sigma$	0.34		1.66/0.66
540.95	$9s/8p\sigma$ [a]	0.25		1.65/0.65
541.00	$10s/9p\sigma$ [a]	0.20		1.67/0.67
541.03	$7s/6p\sigma(001)$ [a]		310	
541.20	IP [b]			

[a]Tentative.
[b]Compare 541.254 eV [20].

breaking and the excitation of the antisymmetric stretching mode due to the vibronic coupling in the O $1s$ excited states of CO_2 have been fully discussed in the analysis of the O $1s$ photoelectron spectra [21–23] and the O $1s$ resonant soft x-ray emission spectra [24–26].

We now discuss the $\Sigma \rightarrow \Sigma$ spectrum in Fig. 2, focusing on the feature observed at 538.7–539.7 eV. With resolving power below 10 000, it was not possible to observe the vibrational structure in this band [18]. Even with resolving power of 10 000, it is nearly impossible to assign all the vibrational structures of this band without resolving the symmetry of the excited states experimentally [20]. In the symmetry-resolved $\Sigma \rightarrow \Sigma$ spectrum at the resolving power of 14 000, however, we can unambiguously extract two vibrational progressions starting at 538.78 and 538.93 eV with vibrational frequencies 250–255 meV. We attribute these progressions to those of the antisymmetric stretching vibrations ν_3 associated with two electronic states $3p\sigma_u$ and $4s\sigma_g$. The lower one starting at 538.78 eV is assigned to $3p\sigma_u$, following the suggestion by Gunnelin *et al.* [32] that the $3p\sigma_u$ resonance occurs at slightly lower energy than the $4s\sigma_g$ resonance.

Transitions to the higher Rydberg orbitals were also observed and assigned to higher members $np\sigma_u$ and $(n+1)s\sigma_g$ as shown in Fig. 2 and listed in Table II. The assignments of these members are straightforward and thus are not discussed further.

We estimate the ionization threshold to be 541.20 eV based on the analysis of the quantum defects. This value is slightly smaller than the reported thresholds [20,33]. The term values and the quantum defects calculated with the present threshold value are also listed in Tables I and II.

C. Analysis of vibrational structure within the linear coupling model

In this section we discuss the vibrational structure in detail. Vibrational structure is observed if the geometry of the molecule changes after electronic excitation. The peak positions and the Franck-Condon factors of the excited vibrations give information on the geometry of the core-excited molecule. To this end, we employ the linear coupling model. This model was originally proposed by Cederbaum and Domcke [34] and has been used successfully in analyses of the vibrational structures both in absorption spectra [35] and in photoelectron spectra [36–38]. The extension of this model to include the antisymmetric stretching mode accompanied by the lowering of symmetry has been done also by Domcke and Cederbaum [21] (see also Ref. [39]).

In the linear coupling model, the harmonic oscillator approximation is employed to express the electronic initial and final states of the transition, and furthermore the vibrational frequencies of the initial and final states are assumed to be identical. Then the Franck-Condon factors for the excitation from $v=0$ in the electronic ground state to the v' vibrational components of the electronic excited state are given by a Poisson distribution:

$$I(0 \rightarrow v') = e^{-S}\frac{S^{v'}}{v'!}. \tag{6}$$

The S factor can be regarded as an average vibrational quantum number for the vibrational excitation. Within the harmonic oscillator approximation, one can show in the present case that

$$S = \frac{K}{2\hbar\omega_3}(\Delta r)^2, \tag{7}$$

where K is the force constant for the antisymmetric stretching vibration mode ν_3, ω_3 is the frequency of the ν_3 vibration in the ground state ($\omega_3 = 291$ meV), and Δr is the change of the CO bond lengths between the initial and final states. One can approximately take account of the change in the frequency between the initial and final states by using the force constant K for the final state [37]. Then the change of the CO bond lengths Δr can be expressed by

$$\Delta r = \left(\frac{2S\hbar}{\omega_3}\frac{m_C + 2m_O}{m_C m_O}\right)^{1/2}\frac{\omega_3}{\omega_3'}, \tag{8}$$

where ω_3' is the frequency of the antisymmetric stretching vibration for the excited state and m_C and m_O are the atomic masses for carbon and oxygen, respectively.

Let us start with the analysis of the $3p\pi_u$ band. The intensity ratio (000):(001):(002) extracted from the peak fitting is 59:34:7. Using Eq. (6) we obtain $S = 0.54$. Inserting this into Eq. (8) we have $\Delta r = 0.056$ Å. This value is in good agreement with $\Delta r = 0.055$ Å reported by Kivimäki *et al.* [22] for the O $1s$ ionized state of CO_2. Note that the increase in the vibrational frequency from $\omega_3 = 291$ meV in the ground state to $\omega_3' = 310$ meV in the excited state corresponds to an increase of the bond strength in the final state. Thus we can expect that the bond lengths are reduced by 0.056 Å in the $3p\pi_u$ core-excited state.

Larger changes in the bond length were found for the $3p\sigma_u$ and $4s\sigma_g$ states. The intensity ratios (000):(001):(002):(003) extracted from the peak fitting are 33:41:21:5 and 53:30:12:5 for $3p\sigma_u$ and $4s\sigma_g$, respectively. We have fitted Eq. (6) to the measured intensities and estimated the S factors to be 1.08 and 0.63, correspondingly. Inserting these S factors into Eq. (8), we obtain the change of the CO bond lengths Δr to be 0.096 and 0.075 Å for $3p\sigma_u$ and $4s\sigma_g$, respectively. Note that the decrease in the vibrational frequency from $\omega_3 = 291$ meV to $\omega_3' = 250–255$ meV corresponds to a decrease of the bond strength in the excited states. Thus we can expect that the bonds are lengthened in the $3p\sigma_u$ and $4s\sigma_g$ core-excited states.

D. Summary

In summary, we have measured the angle-resolved ion-yield spectra of CO_2 in the O $1s$ excitation region with photon-energy-resolving power $E/\Delta E \simeq 14\,000$. Symmetry-resolved spectra were extracted by eliminating the contami-

nation due to overlapping of the $\Sigma \rightarrow \Sigma$ and $\Sigma \rightarrow \Pi$ transitions. The peaks in the symmetry-resolved spectra were assigned to the promotion of an O $1s$ electron to Rydberg orbitals. These Rydberg states were analyzed to obtain the ionization threshold and quantum defects. In addition, vibrational structures were assigned to the antisymmetric stretching vibration caused by the vibronic coupling between the nearly degenerate O $1s$ $1\sigma_g^{-1}np\pi_u$ and O $1s$ $1\sigma_u^{-1}np\pi_u$ states. Franck-Condon analyses within the linear coupling model provide the changes of the C=O bond lengths in the Rydberg states.

[1] A.P. Hitchcock, Phys. Scr. **T31**, 159 (1990).

[2] J. Stöhr, *NEXAFS Spectroscopy* (Springer, Berlin, 1992).

[3] I. Nenner and P. Morin, in *VUV and Soft X-Ray Photoionization*, edited by U. Becker and D. A. Shirley (Plenum Press, New York, 1996), p. 291.

[4] C.T. Chen, Y. Ma, and F. Sette, Phys. Rev. A **40**, 6737 (1989).

[5] F.X. Gadea, H. Köppel, J. Schirmer, L.S. Cederbaum, K.J. Randall, A.M. Bradshaw, Y. Ma, F. Sette, and C.T. Chen, Phys. Rev. Lett. **66**, 883 (1991).

[6] G. Remmers, M. Domke, and G. Kaindl, Phys. Rev. A **47**, 3085 (1993).

[7] J. Schirmer, A.B. Trofimov, K.J. Randall, J. Feldhaus, A.M. Bradshaw, Y. Ma, C.T. Chen, and F. Sette, Phys. Rev. A **47**, 1136 (1993).

[8] N. Saito and I.H. Suzuki, Phys. Rev. Lett. **61**, 2740 (1988).

[9] A. Yagishita, H. Maezawa, M. Ukai, and E. Shigemasa, Phys. Rev. Lett. **62**, 36 (1989).

[10] K. Lee, D.Y. Kim, C.I. Ma, D.A. Lapiano-Smith, and D.M. Hanson, J. Chem. Phys. **93**, 7936 (1990).

[11] E. Shigemasa, K. Ueda, Y. Sato, T. Sasaki, and A. Yagishita, Phys. Rev. A **45**, 2915 (1992).

[12] A. Yagishita, E. Shigemasa, J. Adachi, and N. Kosugi, in *Proceedings of the 10th International Conference on Vacuum Ultraviolet Radiation Physics*, edited by F. J. Wuilleumier, Y. Petroff, and I. Nenner (World Scientific, Singapore, 1993), p. 201.

[13] R.N. Zare, Mol. Photochem. **4**, 1 (1972).

[14] G.E. Busch and K.R. Wilson, J. Chem. Phys. **56**, 3638 (1972).

[15] J.L. Dehmer and D. Dill, Phys. Rev. A **18**, 164 (1978).

[16] N. Kosugi, J. Electron Spectrosc. Relat. Phenom. **79**, 351 (1996).

[17] J. Adachi, N. Kosugi, E. Shigemasa, and A. Yagishita, J. Phys. Chem. **100**, 19783 (1996).

[18] J. Adachi, Y. Takata, E. Shigemasa, N. Kosugi, and A. Yagishita, Photon Factory Activity Rep. **16**, 9 (1999).

[19] J.D. Bozek, N. Saito, and I.H. Suzuki, Phys. Rev. A **51**, 4563 (1995).

[20] K.C. Prince, L. Avaldi, M. Coreno, R. Camilloni, and M. de Simone, J. Phys. B **32**, 2551 (1999).

[21] W. Domcke and L.S. Cederbaum, Chem. Phys. **25**, 189 (1977).

[22] A. Kivimäki, B. Kempgens, K. Maier, H.M. Köppe, M.N. Piancastelli, M. Neeb, and A.M. Bradshaw, Phys. Rev. Lett. **79**, 998 (1997).

[23] N.V. Dobrodey, H. Köppel, and L.S. Cederbaum, Phys. Rev. A **60**, 1988 (1999).

[24] L.S. Cederbaum, J. Chem. Phys. **103**, 562 (1995).

[25] A. Cesar, F. Gel'mukhanov, Y. Luo, H. Ågren, P. Skytt, P. Glans, J. Guo, K. Gunnelin, and J. Nordgren, J. Chem. Phys. **106**, 3439 (1997).

[26] S.A. Malinovskaya and L.S. Cederbaum, Phys. Rev. A **61**, 042706 (2000).

[27] H. Ohashi, E. Ishiguro, Y. Tamenori, H. Kishimoto, M. Tanaka, M. Irie, T. Tanaka, and T. Ishikawa, Nucl. Instrum. Methods Phys. Res. A **467-468**, 529 (2001).

[28] T. Tanaka and H. Kitamura, J. Synchrotron Radiat. **3**, 47 (1996).

[29] H. Ohashi, E. Ishiguro, Y. Tamenori, H. Okumura, A. Hiraya, H. Yoshida, Y. Senba, K. Okada, N. Saito, I.H. Suzuki, K. Ueda, T. Ibuki, S. Nagaoka, I. Koyano, and T. Ishikawa, Nucl. Instrum. Methods Phys. Res. A **467-468**, 533 (2001).

[30] K. Okada, K. Ueda, T. Tokushima, Y. Senba, H. Yoshida, Y. Shimizu, M. Simon, H. Chiba, H. Okumura, Y. Tamenori, H. Ohashi, N. Saito, S. Nagaoka, I.H. Suzuki, E. Ishiguro, I. Koyano, T. Ibuki, and A. Hiraya, Chem. Phys. Lett. **326**, 314 (2000).

[31] K. Ueda, H. Yoshida, Y. Senba, K. Okada, Y. Shimizu, H. Chiba, H. Ohashi, Y. Tamenori, H. Okumura, N. Saito, S. Nagaoka, A. Hiraya, E. Ishiguro, T. Ibuki, I.H. Suzuki, and I. Koyano, Nucl. Instrum. Methods Phys. Res. A **467-468**, 1502 (2001).

[32] K. Gunnelin, P. Glans, P. Skytt, J.-H. Guo, J. Nordgren, and H. Ågren, Phys. Rev. A **57**, 864 (1998).

[33] T.D. Thomas and R.W. Shaw, J. Electron Spectrosc. Relat. Phenom. **5**, 1081 (1974).

[34] L.S. Cederbaum and W. Domcke, J. Chem. Phys. **64**, 603 (1976).

[35] H. Rabus, D. Arvanitis, M. Domke, and K. Baberschke, J. Chem. Phys. **96**, 1560 (1992).

[36] W. Domcke and L.S. Cederbaum, J. Chem. Phys. **64**, 612 (1976).

[37] S.J. Osborne, S. Sundin, A. Ausmees, S. Svensson, L.J. Saethre, O. Svaeren, S.L. Sorensen, J. Végh, J. Karvonen, S. Aksela, and A. Kikas, J. Chem. Phys. **106**, 1661 (1997).

[38] L.J. Sæthre, O. Sværen, S. Svensson, S. Osborne, T.D. Thomas, J. Jauhiainen, and S. Aksela, Phys. Rev. A **55**, 2748 (1997).

[39] T.D. Thomas, L.J. Saethre, S.L. Sorensen, and S. Svensson, J. Chem. Phys. **109**, 1041 (1998).